Design of robust decentralised controllers for MIMO plants with delays through network structure exploitation

Deesh Dileep, Ruben van Parys, Goele Pipeleers, Laurentiu Hetel, Jean-Pierre Richard, Wim Michiels

Design of robust decentralised controllers for MIMO plants with delays through network structure exploitation

Deesh Dileep [a]*, Ruben Van Parys [b], Goele Pipeleers [b], Laurentiu Hetel [c], Jean-Pierre Richard [d] and Wim Michiels [a].

[a]Department of Computer Science, KU Leuven, Belgium, deesh.dileep@cs.kuleuven.be,wim.michiels@cs.kuleuven.be;
[b] Department of Mechanical Engineering, KU Leuven, Belgium, ruben.vanparys@kuleuven.be, goele.pipeleers@mech.kuleuven.be;
[c] University of Lille, UMR 9189 - CRIStAL, CNRS, Centrale Lille, France, laurentiu.hetel@ec-lille.fr;
[d] University of Lille, UMR 9189 - CRIStAL, CNRS, Inria, Centrale Lille, France, jean-pierre.richard@ec-lille.fr.

ARTICLE HISTORY
Compiled December 5, 2018

* corresponding author

ABSTRACT
A methodology is proposed for the design of robust structurally constrained controllers for linear time-delay systems, focusing on decentralised and overlapping fixed-order controllers for Multiple Input Multiple Output (MIMO) systems. The methodology is grounded in a direct optimisation approach and relies on the minimisation of the spectral abscissa and $\mathcal{H}_\infty$ cost functions, as a function of the controller or design parameters. First, an approach applicable to generic MIMO time-delay systems is presented, which is based on imposing a suitable sparsity pattern with the possibility of fixing elements in the controller parameterisation. Second, we show that if the delay system to be controlled has by itself the structure of a network of coupled identical subsystems, this structure can then be exploited by an improved algorithm for the design of decentralised (or overlapping) fixed-order controllers for the infinite-dimensional system, thereby increasing the computational efficiency and scalability with the number of subsystems. The two approaches, which have been implemented in a publicly available software, support system models in terms of delay differential algebraic equations. They allow to model interconnected systems in a systematic way, and include retarded and neutral systems with delays in state, inputs and outputs. Several numerical examples illustrate the effectiveness of the methodology, as well as its extension towards consensus type problems.

KEYWORDS
robust control, structured controllers, time-delay systems, large-scale interconnected systems.

1. Introduction

In this paper we address the design of structurally constrained stabilising and $\mathcal{H}_\infty$ optimal controllers for large-scale linear systems with time-delays, including systems having a network structure. Time-delays are present in the system model as the transfer of energy, material or information is usually not instantaneous. They appear, for instance, as computation and communication lags, they model the transport phenomena and heredity, and arise as feedback delays in control loops (Michiels, Hilhorst, Pipeleers, Vyhlídal, & Swevers, 2017). For large-scale multiple-input, MIMO systems, it is often infeasible or costly to implement centralised controllers (see (Siljak, 1991), (Lunze, 1992) and references within). As a consequence, structurally constrained controllers, in particular decentralised or distributed (PID) controllers, are favourable for industrial applications (McMillan, 2012).

Traditional methods for designing stabilising and optimal $\mathcal{H}_\infty$ controllers for linear time-invariant (LTI) MIMO are grounded in the Riccati equation and linear matrix inequality (LMI) framework (see (Gahinet & Apkarian, 1994), (Fridman, 2014), and references therein). In general, controllers designed by these methods are not structured and their dimension is equal or larger than the order of the plant. The problem addressed in this paper is characterised by two main challenges. First, with the aforementioned approaches imposing constraints on the structure or order of the controller gives rise to non-convex bi-linear matrix inequalities, which are difficult to solve. Second, by including delays the system models become infinite-dimensional (Michiels et al., 2017), hence, any controller design problem involving tuning of finitely many controller parameters can be considered as a reduced-order controller design problem.

The methodology used in this paper is grounded in the direct optimisation approach for controller design, where objective functions specifying performance criteria are directly optimised as a function of the available controller or design parameters. More specifically, the stabilisation and robust controller design problem for the delay system are translated into solving the, in general, non-smooth non-convex optimisation problems of minimising the spectral abscissa function and $\mathcal{H}_\infty$ norms (see (Michiels, 2011) and (Gumussoy & Michiels, 2011) respectively) using dedicated optimisation algorithms. This approach generalises the one underlying the HIFOO package (Burke, Henrion, Lewis, & Overton, 2006) and the one underlying the MATLAB function `hinfstruct` (Apkarian & Noll, 2006), both for finite-dimensional LTI systems.

The subject-matter of this paper is two-fold. First, the direct optimisation approach for designing fixed-order $\mathcal{H}_\infty$ optimal controller for time-delay systems is extended towards a more general class of structured controllers for MIMO systems, which includes decentralised and overlapping controllers (recalling from (Dileep, Michiels, Hetel, & Richard, 2018)). We assume that controllers are overlapping when they consider measured output from neighbouring subsystems. Hereby the structural constraints are translated into sparsity patterns for the controller parameterisation, as done in (Ozer & Iftar, 2015) for the stabilisation problem. The approach starts from a state space representation and fully exploits properties of delay systems. Particularly for neutral type systems with multiple delays, it explicitly takes into account the fragility (problem) of potential sensitivity of the spectral abscissa and $\mathcal{H}_\infty$ norms with respect to infinitesimal delay perturbations (Hale & Verduyn Lunel, 2002; Michiels, Vyhlídal, Ziték, Nijmeijer, & Henrion, 2009). The adopted approach complements the generic approach for infinite-dimensional systems in (Apkarian & Noll, 2017), which is based on appropriately sampling the frequency response. Finally we notice that the tuning of decentralised PID controller for flexible structures in (Shi, Davison, Kwong, &

Davison, 2016) also falls within the direct optimisation approach. We also point to (Alavian & Rotkowitz, 2015, 2013) and the references therein, where it is shown how for particular combinations of LTI plants and admissible controllers, the $\mathcal{H}_\infty$ design problem can still be recast as a convex optimisation problem.

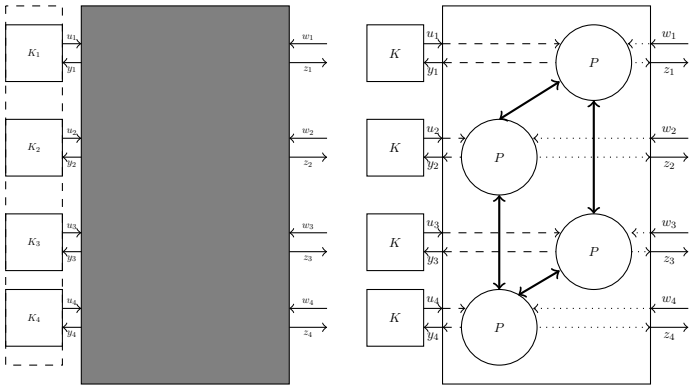

(a) MIMO plant and structurally constrained controller.

(b) Structured plant with identical subsystems and controllers.

Figure 1. Classes of systems under consideration. Section 3.3 presents an approach for the design of structured controllers for generic MIMO systems (shown in Fig. 1a for the special case of decentralised feedback control). In Section 4 an improved approach is presented for a class of systems having a network structure (Fig. 1b).

Second, as the main contribution we consider systems which have themselves a network structure, and show how in the design of classes of decentralized and distributed fixed-order controllers the structure of the overall system can be exploited by a refined method, in order to arrive at a higher computational efficiency, and improved scalability with respect to the number of subsystems. More precisely, we will assume that the MIMO system consists of a network of coupled identical subsystems, each of them having an identical local controller to be designed. The key will be a decoupling transformation reducing the overall design problem into a robust/simultaneous controller design problem for one parameterised subsystem, where the allowable values of the parameter are related to the adjacency matrix of the network graph. The same kind of transformation has been used for the design of full order distributed controllers for delay-free systems in (Massioni & Verhaegen, 2009), within an LMI framework. It has also proven its usefulness in the analysis of linear consensus problems (see, e.g. (Olfati-Saber & Murray, 2004) and the references therein), and of network synchronisation, as it lays at the basis of the so-called Master Stability Function (Pecora & Carroll, 1998).

The presented algorithms for structurally constrained controller design, with the possibility of network exploitation, have been integrated in the existing software tool `tds_hopt` for fixed-order $\mathcal{H}_\infty$ optimisation of delay systems corresponding to the article (Gumussoy & Michiels, 2011). The improved software tool (`tds_hopt-nse`, see (Dileep & Michiels, 2018)) allows the designer to select the sub-controller input-output interactions and specify their orders. Additionally, the user can also specify the adjacency matrix and other matrices corresponding to the input or output signals exchanged between coupled subsystems.

Both presented methods start from system models in terms of linear delay-differential algebraic equations (DDAEs), which are very flexible and general as they allow a systematic description of (sub)-systems, controllers and their interconnections.

Furthermore, as we shall see in Section 2, DDAE models include delay systems of both retarded and neutral type and preserve linearity of system matrices with respect to the controller parameters in the closed-loop system description. We will also illustrate how, relying on the DDAE framework mentioned above, the applicability of the design method can be extended towards synchronisation and consensus type problems in networks of delay-coupled systems. This involves the design of feedback controllers acting on output measurements, relative with respect to the output of other subsystems. The targeted classes of systems, related to the two main contributions mentioned above, are illustrated in Fig. 1.

The remainder of the paper is organised as follows. Section 2 introduces the class of DDAE models and Section 3 reviews the direct optimisation approach for designing fixed-order controllers for time-delay systems. In Section 3.3, its extension towards the design of structurally constrained controllers, focusing on decentralised and overlapping controllers, is presented (recalling from (Dileep et al., 2018)). Section 4 addresses the main contribution for networks of interconnected systems, and the exploitation of the network structure. Some numerical examples are presented in Section 5, where as an example of a consensus-type problem, the control of a model for a platoon of vehicles is considered. Finally, some concluding remarks are given in Section 6.

2. Preliminaries

In this work we consider plants described by delay differential algebraic equations

$$\mathcal{P}: \begin{cases} E_p \dot{x}_p(t) & = A_{p0} x_p(t) + \sum_{i=1}^{m} A_{pi} x_p(t-\tau_i) + B_{p1} u(t) + B_{p2} w(t), \\ y(t) & = C_{p1} x_p(t), \\ z(t) & = C_{p2} x_p(t), \end{cases} \tag{1}$$

where $x_p(t) \in \mathbb{R}^{n_p}$ is the instantaneous state vector at time t. Similarly, $u(t) \in \mathbb{R}^{n_u}$ and $y(t) \in \mathbb{R}^{n_y}$ are instantaneous controlled input and measured output vectors at time t, whereas the instantaneous exogenous input and the instantaneous exogenous (or controlled) output are represented as $w(t) \in \mathbb{R}^{n_w}$ and $z(t) \in \mathbb{R}^{n_z}$ respectively. We use the notations $\mathbb{R}$, $\mathbb{R}^+$ and $\mathbb{R}_0^+$ to represent sets of real numbers, non-negative real numbers and strictly positive real numbers respectively, and $x_p \in \mathbb{R}^{n_p}$ is a short notation for $(x_{p1}, ..., x_{pn_p})$. There are m distinct time-delays present in the state vector, where m is a positive integer. Throughout this paper, A, B, C, D and E (with or without subscript) will be used to represent constant real-valued matrices. We allow the leading matrix E_p in (1) to be singular. The time-delays satisfy $0 < \tau_i \leq \tau_{\max}$.

Even without the presence of the feed-through terms, input delays or output delays, the model given by (1) allows to describe LTI systems with discrete delays in their most general form, including systems of retarded and neutral type, delays in input and output, non-trivial feed-through, and delayed interconnections of subsystems. This is portrayed with the help of a simple example below (we refer to (Dileep et al., 2018) for more examples). Furthermore, as differential equations and algebraic equations modelling connections can be directly included in (1), the latter is very amendable for modelling interconnected systems.

Example 2.1. Let us consider the presence of time-delays at the controlled input, the measured output and the first-order derivative of the state vector in an LTI system (a

neutral type time-delay system),

$$\begin{cases} \dot{\psi}(t) + e_1\dot{\psi}(t-\phi) &= a\psi(t) + b_0u(t) + b_1u(t-\bar{\phi}), \\ y(t) &= c_0\psi(t) + c_1\psi(t-\hat{\phi}) + du(t), \end{cases} \tag{2}$$

where a, b_0, b_1, e_1, d, c_0 and c_1 are constants, $\phi, \bar{\phi}$ and $\hat{\phi}$ are constant time-delays, ψ is the state, u is the input, and y is the output. Using dummy variables γ_ψ, γ_u and γ_y, we can rewrite the system as

$$\begin{aligned} \dot{\gamma_\psi}(t) &= a\psi(t) + b_0\gamma_u(t) + b_1\gamma_u(t-\bar{\phi}), \\ 0 &= -\gamma_\psi(t) + \psi(t) + e_1\psi(t-\phi), \\ 0 &= -\gamma_u(t) + u(t), \\ 0 &= -\gamma_y(t) + c_0\psi(t) + c_1\psi(t-\hat{\phi}) + d\gamma_u(t), \\ y(t) &= \gamma_y(t). \end{aligned} \tag{3}$$

The dummy variables γ_ψ, γ_u and γ_y , defined by the 2^{nd}-4^{th} equations in (3), allow to move a delay in the derivative of the state variable (inherent to a neutral type system), in the input and the output to a delay in a (pseudo) state variable, and then remove the feed-through term from the output equation. That is, by defining the new state vector as $x_p(t) = [\gamma_\psi^{\mathrm{T}}(t)\ \psi^{\mathrm{T}}(t)\ \gamma_u^{\mathrm{T}}(t)\ \gamma_y^{\mathrm{T}}(t)]^{\mathrm{T}}$, the LTI system (2) can be turned into form (1). ∘

The system described in (1) can be controlled using a feedback controller with prescribed order "n_c",

$$\mathcal{K} : \begin{cases} \dot{x}_c(t) = A_cx_c(t) + B_cy(t), \\ u(t) = C_cx_c(t) + D_cy(t), \end{cases} \tag{4}$$

where $x_c(t) \in \mathbb{R}^{n_c}$ is the controller state vector. Here, the case of $n_c = 0$ corresponds to a static or proportional controller of the form $u(t) = D_c\ y(t)$. The other cases of $n_c \geq 1$ corresponds to that of a dynamic controller as given in (4), where A_c is a matrix of size $n_c \times n_c$.

The feedback interconnection of plant (1) and controller (4) can be described, when defining $x = [x_p^{\mathrm{T}}u^{\mathrm{T}}\gamma_w^{\mathrm{T}}x_c^{\mathrm{T}}y^{\mathrm{T}}]^{\mathrm{T}}$, by the following DDAE,

$$\begin{cases} E\dot{x}(t) &= A_0x(t) + \sum_{i=1}^{m} A_ix(t-\tau_i) + Bw(t), \\ z(t) &= Cx(t), \end{cases} \tag{5}$$

where

$$E = \begin{bmatrix} E_p & 0 & 0 & 0 & 0 \\ 0 & 0 & 0 & 0 & 0 \\ 0 & 0 & 0 & 0 & 0 \\ 0 & 0 & 0 & I & 0 \\ 0 & 0 & 0 & 0 & 0 \end{bmatrix},\ A_0 = \begin{bmatrix} A_{p0} & B_{p1} & B_{p2} & 0 & 0 \\ C_{p1} & 0 & 0 & 0 & -I \\ 0 & 0 & -I & 0 & 0 \\ 0 & 0 & 0 & A_c & B_c \\ 0 & -I & 0 & C_c & D_c \end{bmatrix}. \tag{6}$$

and

$$A_i = \begin{bmatrix} A_{pi} & 0 & 0 & 0 & 0 \\ 0 & 0 & 0 & 0 & 0 \\ 0 & 0 & 0 & 0 & 0 \\ 0 & 0 & 0 & 0 & 0 \\ 0 & 0 & 0 & 0 & 0 \end{bmatrix}, \; B = \begin{bmatrix} 0 \\ 0 \\ I \\ 0 \\ 0 \end{bmatrix}, \; C^{\mathrm{T}} = \begin{bmatrix} C_{p2} \\ 0 \\ 0 \\ 0 \\ 0 \end{bmatrix}.$$

The price to pay for the generality of system description (1) is that also classes of non-causal systems and systems with impulsive solutions are included. For the former, consider as an example system

$$\begin{cases} \dot{x}_1(t) &= -x_1(t) + x_2(t), \\ 0 &= x_1(t) + x_2(t-2). \end{cases}$$

In order to exclude such systems, in the remainder of the paper we take the following assumption for well-posedness which is satisfied in most practical cases of interest.

Assumption 1. Matrix $U^T(A_{p0} + B_{p1}D_cC_{p1})V$ is invertible, where the columns of U and V form a minimal basis for the left and right null space of matrix E_p respectively.

This assumption, which corresponds to a rephrasing of Assumption 3.1 in (Gumussoy & Michiels, 2011) (see appendix for proof), ensures that DDAE (1) without inputs is semi-explicit (differentiation index equal to 1), and that this property is not altered by the feedback. We refer to (Gumussoy & Michiels, 2011) for more details. Throughout this paper, we assume that plants of the form (1) can be stabilised using a fixed-order controller of the form (4).

3. Fixed-order controller design

We build on the approach of (Michiels, 2011), (Gumussoy & Michiels, 2011) and (Dileep et al., 2018) to stabilise and subsequently optimise the robustness of the closed-loop system. We directly optimise stability and performance measures as a function of the parameter vector $\boldsymbol{p}$, containing the tunable parameters of the controller, that is,

$$\boldsymbol{p} = \mathrm{vec}\left(\left[\begin{array}{c|c} A_c & B_c \\ \hline C_c & D_c \end{array}\right] \right) \tag{7}$$

for a non-structured controller of dimension n_c.The objective functions used for optimisation of the controller parameters are described in the following subsections.

3.1. Robust spectral abscissa optimisation

The spectral abscissa of the closed-loop system (5) with $w \equiv 0$ is defined as follows,

$$c(\boldsymbol{p}; \boldsymbol{\tau}) = \sup_{\lambda \in \mathbb{C}} \{\Re(\lambda) : \det\Delta(\lambda, \boldsymbol{p}; \boldsymbol{\tau}) = 0\}, \tag{8}$$

where

$$\Delta(\lambda, \boldsymbol{p}; \boldsymbol{\tau}) = \lambda E - A_0(\boldsymbol{p}) - \sum_{i=1}^{m} A_i \mathrm{e}^{-\lambda \tau_i},$$

$\boldsymbol{\tau} \in (\mathbb{R}_0^+)^m$ is the vector of system time-delays, and $\Re(\lambda)$ is the real part of the complex number λ. We use the notation $m(a; b)$ throughout this paper to indicate m as a function of variable a, depending on parameter b. The exponential stability of the null solution of (5) is determined by the condition $c(\boldsymbol{p}; \boldsymbol{\tau}) < 0$ (see (Michiels, 2011)). However, the function $\boldsymbol{\tau} \mapsto c(\boldsymbol{p}; \boldsymbol{\tau})$ might not be continuous and could be sensitive to infinitesimal delay changes (in general, as neutral time-delay system could be included in model (1)). Therefore, we define the *robust spectral abscissa* $C(\boldsymbol{p}; \boldsymbol{\tau})$ as in the following way,

$$C(\boldsymbol{p}; \boldsymbol{\tau}) := \lim_{\epsilon \to 0+} \sup_{\boldsymbol{\tau}_\epsilon \in \mathcal{B}(\boldsymbol{\tau}, \epsilon)} c(\boldsymbol{p}; \boldsymbol{\tau}_\epsilon). \tag{9}$$

In (9), $\mathcal{B}(\boldsymbol{\tau}, \epsilon)$ is an open ball of radius $\epsilon \in \mathbb{R}^+$ centered at $\boldsymbol{\tau}$, $\mathcal{B}(\boldsymbol{\tau}, \epsilon) := \{\bar{\theta} \in \mathbb{R}^m : ||\bar{\theta} - \boldsymbol{\tau}|| < \epsilon\}$. The sensitivity of the spectral abscissa with respect to infinitesimal delay perturbations has been resolved by considering the robust spectral abscissa, since this function can be shown to be a continuous function of the delay parameters (and also parameters in $\boldsymbol{p}$), see (Michiels, 2011). We now define the concept of strong exponential stability.

Definition 1: The null solution of (5) when $w \equiv 0$ is strongly exponentially stable if there exists a number $\epsilon > 0$ such that the null solution of

$$E\dot{x}(t) = A_0 x(t) + \sum_{i=1}^{m} A_i x(t - (\tau_i + \delta\tau_i)))$$

is exponentially stable for all $\delta\boldsymbol{\tau} \in \mathbb{R}^m$ satisfying $||\delta\boldsymbol{\tau}|| < \epsilon$ and $\tau_i + \delta\tau_i \geq 0,\ i = 1, ..., m$.

In (Michiels, 2011) it has been shown that the null solution is strongly exponentially stable iff $C(\boldsymbol{p}) < 0$. Note that we stress the dependence of functions on $\boldsymbol{\tau}$ only when necessary. However, for the optimisation problem, the objective function only has controller parameters ($\boldsymbol{p}$) as variables. To obtain a strongly exponentially stable closed-loop system and to maximise the exponential decay rate of the solutions, the tunable controller parameters (in $\boldsymbol{p}$) are optimised for minimum robust spectral abscissa, that is, they are obtained by minimising

$$\min_{\boldsymbol{p}} C(\boldsymbol{p}). \tag{10}$$

3.2. Strong $\mathcal{H}_\infty$ norm optimisation

The transfer function from w to z of the system represented by (5) is given by

$$G(\lambda, \boldsymbol{p}; \boldsymbol{\tau}) := C\Big(\lambda E - A_0(\boldsymbol{p}) - \sum_{i=1}^{m} A_i \mathrm{e}^{-\lambda \tau_i}\Big)^{-1} B. \tag{11}$$

Under assumption of internal stability, the $\mathcal{H}_\infty$ norm of the transfer function given in (11) can be expressed as

$$||G(j\omega, \boldsymbol{p}; \boldsymbol{\tau})||_{\mathcal{H}_\infty} = \sup_{\omega \in \mathbb{R}} \sigma_1(G(j\omega, \boldsymbol{p}; \boldsymbol{\tau})). \tag{12}$$

However, similar to the spectral abscissa function, the function $\boldsymbol{\tau} \in (\mathbb{R}_0^+)^m \mapsto ||G(j\omega, \boldsymbol{p}; \boldsymbol{\tau})||_{\mathcal{H}_\infty}$ might not be continuous and could be sensitive to infinitesimal delay changes (in general, inherited from the behaviour of the transfer function at high frequencies). Therefore, under the assumption of strong exponential stability of the null solution, we define the strong $\mathcal{H}_\infty$ norm $|||G(j\omega, \boldsymbol{p}; \boldsymbol{\tau})|||_{\mathcal{H}_\infty}$.

$$|||G(j\omega, \boldsymbol{p}; \boldsymbol{\tau})|||_{\mathcal{H}_\infty} := \lim_{\epsilon \to 0+} \sup_{\boldsymbol{\tau}_\epsilon \in \mathcal{B}(\boldsymbol{\tau}, \epsilon)} ||G(j\omega, \boldsymbol{p}; \boldsymbol{\tau}_\epsilon)||_{\mathcal{H}_\infty} \tag{13}$$

Contrary to the (standard) $\mathcal{H}_\infty$ norm, the strong $\mathcal{H}_\infty$ norm continuously depends on the delay parameter. The continuous dependence also holds with respect to the elements of the system matrices, which include the elements in $\boldsymbol{p}$, as shown in (Gumussoy & Michiels, 2011).
To improve robustness or performance expressed in terms of the $\mathcal{H}_\infty$ norm of (12), tunable controller parameters (in $\boldsymbol{p}$) can be optimised by solving the problem

$$\min_{\boldsymbol{p}} |||G(j\omega, \boldsymbol{p})|||_{\mathcal{H}_\infty}. \tag{14}$$

Finally, recall that if the closed-loop system corresponds to a delay system of retarded type, the robust spectral abscissa and strong $\mathcal{H}_\infty$ norm reduce to the standard spectral abscissa and $\mathcal{H}_\infty$ norm (see (Michiels, 2011) and (Gumussoy & Michiels, 2011)).

3.3. Design of structurally constrained controllers

Several kinds of structurally constrained controllers can be obtained by enforcing constraints on elements of the controller matrices contained in

$$P_M := \left[\begin{array}{c|c} A_c & B_c \\ \hline C_c & D_c \end{array}\right]$$

and only use the free parameters as variables in the optimisation problem described in the previous section (see (Dileep et al., 2018) for more details). For decentralised and overlapping controllers this amounts to introducing a sparsity pattern, as can be portrayed with the help of the following example.

Example 3.1. Consider a MIMO system containing two control inputs and two measured outputs, and a controller parameterised in the following way:

$$\begin{bmatrix} \dot{x}_{c1} \\ \dot{x}_{c2} \\ u_1 \\ u_2 \end{bmatrix} = \overbrace{\left[\begin{array}{cc|cc} a_{c_{11}} & 0 & b_{c_{11}} & 0 \\ 0 & a_{c_{22}} & \boxed{b_{c_{21}}} & b_{c_{22}} \\ \hline c_{c_{11}} & 0 & d_{c_{11}} & 0 \\ 0 & c_{c_{22}} & \boxed{d_{c_{21}}} & d_{c_{22}} \end{array}\right]}^{P_M} \begin{bmatrix} x_{c1} \\ x_{c2} \\ y_1 \\ y_2 \end{bmatrix}. \tag{15}$$

The controller is of order 2 ($n_c = 2$), however, two sub-controllers of order 1 are present. We can observe that if the elements b_{c21} and d_{c21} are set be zero, we have decentralised sub-controllers, that is, interactions between their states, inputs, and outputs are decoupled. If elements b_{c21} and d_{c21} are non-zero, the sub-controllers are overlapping, that is, the input and sub-controller state interactions are decoupled, but one of the measured output is shared between the two sub-controllers. ∘

The sparsity pattern can be described by a binary matrix F_M of the same dimensions as P_M, whose (i, j)-th element satisfies

$$f_{Mij} = \begin{cases} 0, & \text{if } p_{Mij} \text{ is an optimisation variable;} \\ 1, & \text{if } p_{Mij} \text{ is a fixed element.} \end{cases} \tag{16}$$

This allows us to redefine the parameter vector from (7) to include only the non-zero/non-fixed elements using information in F_M,

$$\boldsymbol{p} = \underset{F_M}{\operatorname{vec}} P_M = \underset{F_M}{\operatorname{vec}} \left[\begin{array}{c|c} A_c & B_c \\ \hline C_c & D_c \end{array}\right], \tag{17}$$

where $\operatorname{vec}_{F_M} P_M$ is a vector containing the elements of P_M for which the corresponding element in F_M is equal to one, keeping the same order as in $\operatorname{vec} P_M$.

In the MATLAB tool corresponding to this article (Dileep & Michiels, 2018), the user has the option to either specify F_M directly, or, for the case of decentralised and overlapping controllers, specify two interaction matrices M_{C_u} and M_{C_y}. These matrices denote the interaction between input, output and sub-controllers, The controller parameters (in $\boldsymbol{p}$) can also be optimised for the function $f_o(\boldsymbol{p})$,

$$f_o(\boldsymbol{p}) = \begin{cases} \infty, & \text{if } \; C(\boldsymbol{p}) \geq 0, \\ \alpha \; C(\boldsymbol{p}) + \; (1-\alpha) \; |||G(j\omega, \boldsymbol{p})|||_{\mathcal{H}_\infty}, & \text{if } \; C(\boldsymbol{p}) < 0. \end{cases} \tag{18}$$

Here $0 \leq \alpha \leq 1$ is the weight used for linear combination of the objective functions. The two objective functions in this combination are in general non-convex. They may be not-everywhere differentiable, even not-everywhere Lipschitz continuous, see (Gumussoy & Michiels, 2011; Michiels, 2011) where using the same approach (unstructured) fixed-order controllers are designed. In our implementation the HANSO code (Hybrid Algorithm for Non-smooth Optimisation, see (Overton, 2009)) is used for solving the optimisation tasks. The algorithm relies on a routine for the computation of the considered objective function as well as its gradient whenever the objective function is differentiable. The value of the objective function is obtained by computing rightmost eigenvalues of the DDAE for the spectral abscissa, and by a generalisation of the Boyd-Balakrishnan-Kabamba (Boyd, Balakrishnan, & Kabamba, 1989) / Bruinsma-Steinbuch (Bruinsma & Steinbuch, 1990) algorithm for the $\mathcal{H}_\infty$ norm, relying on computing imaginary axis solutions of an associated Hamiltonian eigenvalue problem. It typically constitutes the dominant computational cost in every iteration. On the contrary, derivatives of the objective functions with respect to controller parameters are obtained at a negligible cost from left and right eigenvectors. By this property and by the fact that fixed-order controllers of lower order are desirable for application, reducing the number of variables beyond the imposed structure, e.g., by working with canonical forms, does not have a considerable impact on the overall

computational cost. We refer to (Gumussoy & Michiels, 2011; Michiels, 2011) and the references therein for more information on the previously described algorithmic components.
A strongly exponentially stable closed-loop system is required to start the optimisation of objective functions involving the strong $\mathcal{H}_\infty$ norm. If this is not the case, a preliminary stabilisation phase is performed based on optimising the robust spectral abscissa. Due to the non-convexity of the objective functions, there is no guarantee of convergence to the global minimum. In our software, this is addressed by using randomly generated initial values for the controller parameters, along with initial controllers specified by the user, and choosing the best solution from them.

Remark. It is also possible to design other type of controllers by imposing sparsity or fixing elements in the parameterisation of the unstructured controller. A kind of distributed controller can be considered by including the off-diagonal blocks (or elements) of the A_c matrix in the vector $\boldsymbol{p}$. In (Dileep et al., 2018), structural constraints in a dynamic controller were used to represent a PID controller. $\diamond$

4. Exploiting network structure of systems

We improve the generic approach presented in Section 3.3 for the case of designing a decentralised (or overlapping) controller for a special class of systems. These systems have some network structure, consisting of identical subsystems to be controlled by identical local controllers, see Fig. 1b.

More precisely, we consider a network described by a directed graph $\mathcal{G} = \{\mathcal{V}, \mathcal{E}, A_M\}$ with a set of nodes $\mathcal{V} = \{1, 2, 3, ..., n\}$ and a set of edges $\mathcal{E} \subset \mathcal{V} \times \mathcal{V}$. The edge $(i, j) \in \mathcal{E}$ connects from node $j \in \mathcal{V}$ to node $i \in \mathcal{V}$. The graph $\mathcal{G}$ need not be strongly connected. However, we assume that the graph is simple, which means that there is no self coupling. We denote by

$$A_M = [a_{Mij}]_{i,j=1}^{n}$$

the weighted adjacency matrix with zero diagonal entries and non-negative off-diagonal entries such that $a_{Mij} > 0$ if and only if the corresponding edge $(i, j) \in \mathcal{E}$.

Each of the n nodes hosts a dynamical system described by a DDAE as

$$\begin{cases} \hat{E}_p \dot{x}_{pi}(t) = & \hat{A}_{p0} x_{pi}(t) + \sum_{k=1}^{m} \hat{A}_{pk} x_{pi}(t - \tau_k) + \hat{B}_{p1} u_i(t) + \hat{B}_{p2} w_i(t) + \hat{B}_{p3} u_{ci}(t), \\ y_i(t) = & \hat{C}_{p1} x_{pi}(t), \\ z_i(t) = & \hat{C}_{p2} x_{pi}(t), \\ y_{ci}(t) = & \hat{C}_{p3} x_{pi}(t), \qquad i = 1, \ldots, n, \end{cases} \tag{19}$$

where $x_{pi} \in \mathbb{R}^{\hat{n}_p}$ is the state, $u_i \in \mathbb{R}^{\hat{n}_u}$ is the controlled input, $y_i \in \mathbb{R}^{\hat{n}_y}$ is the measured output, $w_i \in \mathbb{R}^{\hat{n}_w}$ is the exogenous input, and $z_i \in \mathbb{R}^{\hat{n}_z}$ is the exogenous output of node "i". The additional input $u_{ci} \in \mathbb{R}^{n_{uc}}$ and output $y_{ci} \in \mathbb{R}^{n_{yc}}$ are related to the coupling with other nodes/subsystems in the network, described by

$$u_{ci}(t) = \sum_{j=1}^{n} a_{Mij} y_{cj}(t), \quad i = 1, \ldots, n. \tag{20}$$

For the same reason as that of (1), (19) is in the most general DDAE form ($\hat{E}_p$ can be singular). We consider the case where a system of the form (1) is composed of subsystems of the form (19) and (20). We assume that each subsystem is controlled using a fixed-order LTI feedback controller of the form

$$\begin{cases} \dot{x}_{ci}(t) = \hat{A}_c x_{ci}(t) + \hat{B}_c y_i(t), \\ u_i(t) = \hat{C}_c x_{ci}(t) + \hat{D}_c y_i(t). \end{cases} \tag{21}$$

Defining $x_i(t) = [x_{pi}^{\mathrm{T}}(t)\ u_i^{\mathrm{T}}(t)\ \gamma_{w_i}^{\mathrm{T}}\ x_{ci}^{\mathrm{T}}(t)\ y_i^{\mathrm{T}}(t)]^{\mathrm{T}}$, the closed-loop system state $x_i \in \mathbb{R}^{n_{cl}}$ which includes the plant and controller can be written in the DDAE form as

$$\begin{cases} \hat{E}\dot{x}_i(t) & = \hat{A}_0 x_i(t) + \sum_{k=1}^{m} \hat{A}_k x_i(t-\tau_k) + \sum_{j=1}^{n} a_{Mij} \hat{B}\hat{C} x_j(t) + \hat{B}_2 w_i(t) \\ z_i(t) & = \hat{C}_2 x_i(t), \qquad\qquad i = 1, \ldots, n, \end{cases} \tag{22}$$

where

$$\hat{E} = \begin{bmatrix} \hat{E}_p & 0 & 0 & 0 & 0 \\ 0 & 0 & 0 & 0 & 0 \\ 0 & 0 & 0 & 0 & 0 \\ 0 & 0 & 0 & I & 0 \\ 0 & 0 & 0 & 0 & 0 \end{bmatrix}, \hat{A}_0 = \begin{bmatrix} \hat{A}_{p0} & \hat{B}_{p1} & \hat{B}_{p2} & 0 & 0 \\ \hat{C}_{p1} & 0 & 0 & 0 & -I \\ 0 & 0 & -I & 0 & 0 \\ 0 & 0 & 0 & \hat{A}_c & \hat{B}_c \\ 0 & -I & 0 & \hat{C}_c & \hat{D}_c \end{bmatrix} \tag{23}$$

and

$$\hat{A}_k = \begin{bmatrix} \hat{A}_{pk} & 0 & 0 & 0 & 0 \\ 0 & 0 & 0 & 0 & 0 \\ 0 & 0 & 0 & 0 & 0 \\ 0 & 0 & 0 & 0 & 0 \\ 0 & 0 & 0 & 0 & 0 \end{bmatrix} \hat{B} = \begin{bmatrix} \hat{B}_{p3} \\ 0 \\ 0 \\ 0 \\ 0 \end{bmatrix}; \quad \hat{C}^{\mathrm{T}} = \begin{bmatrix} \hat{C}_{p3} \\ 0 \\ 0 \\ 0 \\ 0 \end{bmatrix} \hat{B}_2 = \begin{bmatrix} 0 \\ 0 \\ I \\ 0 \\ 0 \end{bmatrix}; \quad \hat{C}_2^{\mathrm{T}} = \begin{bmatrix} \hat{C}_{p2} \\ 0 \\ 0 \\ 0 \end{bmatrix}.$$

The state-space representation for the overall structured system then takes the form

$$\begin{aligned} I \otimes \hat{E} \begin{bmatrix} \dot{x}_1(t) \\ \dot{x}_2(t) \\ \vdots \\ \dot{x}_n(t) \end{bmatrix} &= I \otimes \hat{A}_0 \begin{bmatrix} x_1(t) \\ x_2(t) \\ \vdots \\ x_n(t) \end{bmatrix} + \sum_{k=1}^{m} I \otimes \hat{A}_k \begin{bmatrix} x_1(t-\tau_k) \\ x_2(t-\tau_k) \\ \vdots \\ x_n(t-\tau_k) \end{bmatrix} \\ &+ A_M \otimes \hat{B}\hat{C} \begin{bmatrix} x_1(t) \\ x_2(t) \\ \vdots \\ x_n(t) \end{bmatrix} + I \otimes \hat{B}_2 \begin{bmatrix} w_1(t) \\ w_2(t) \\ \vdots \\ w_n(t) \end{bmatrix}, \quad \begin{bmatrix} z_1(t) \\ z_2(t) \\ \vdots \\ z_n(t) \end{bmatrix} = I \otimes \hat{C}_2 \begin{bmatrix} x_1(t) \\ x_2(t) \\ \vdots \\ x_n(t) \end{bmatrix}. \end{aligned} \tag{24}$$

In the following subsections, we describe how the model in (24) can be decomposed for stability and robustness optimisation.

4.1. Decoupling for the stabilisation problem

Based on the (complex) Schur decomposition theorem (see (Meyer, 2000)), there always exists a unitary transformation matrix $T \in \mathbb{C}^{n\times n}$ and an upper-triangular matrix $Z \in \mathbb{C}^{n\times n}$ such that

$$TA_MT^{-1} = Z. \tag{25}$$

Note that spectrum of A_M appears on the diagonal of Z. Let us consider the whole system where $w(t) \in \mathbb{R}^{n\cdot\hat{n}_w}$ and $z(t) \in \mathbb{R}^{n\cdot\hat{n}_z}$ are the exogenous input and output respectively, and $x(t) \in \mathbb{R}^{n\cdot n_{cl}}$ and $\bar{x}(t) \in \mathbb{R}^{n\cdot n_{cl}}$ are the state before and after the transformation respectively. Also, $w(t) = [w_1^{\mathrm{T}}(t)\ ...\ w_n^{\mathrm{T}}(t)]^{\mathrm{T}}$, $z(t) = [z_1^{\mathrm{T}}(t)\ ...\ z_n^{\mathrm{T}}(t)]^{\mathrm{T}}$, $x(t) = [x_1^{\mathrm{T}}(t)\ ...\ x_n^{\mathrm{T}}(t)]^{\mathrm{T}}$, and $\bar{x}(t) = [\bar{x}_1^{\mathrm{T}}(t)\ ...\ \bar{x}_n^{\mathrm{T}}(t)]^{\mathrm{T}}$. If we apply the transformation using $\hat{T}$ (that is, $x(t) = \hat{T}^{-1}\bar{x}(t)$) to (24), where $\hat{T} = T \otimes I$, we obtain the equation

$$\begin{aligned}(I\otimes\hat{E})\dot{\bar{x}}(t) &= (I\otimes\hat{A}_0)\bar{x}(t) + \sum_{k=1}^{m}(I\otimes\hat{A}_k)\bar{x}(t-\tau_k) + (Z\otimes\hat{B}\hat{C})\bar{x}(t)\\ &\quad + \underbrace{\hat{T}(I\otimes\hat{B}_2)}_{(I\otimes\hat{B}_2)\hat{T}} w(t), \quad z(t) = \underbrace{(I\otimes\hat{C}_2)\hat{T}^{-1}}_{\hat{T}^{-1}(I\otimes\hat{C}_2)}\ \bar{x}(t).\end{aligned} \tag{26}$$

Note that this transformation does not affect $\hat{A}_0$, $\hat{A}_k$ or $\hat{E}$ because of the property

$$\hat{T}(I\otimes\hat{A}_0)\hat{T}^{-1} = (T\otimes I)(I\otimes\hat{A}_0)(T^{-1}\otimes I) = TT^{-1}\otimes\hat{A}_0.$$

Observing that for zero exogenous input, (26) has a cascaded structure, the following theorem directly follows.

Theorem 4.1. *Let the spectrum of A_M be denoted by $\{\lambda_{a1},\ldots,\lambda_{am}\}$. System (26) with $w \equiv 0$ is exponentially stable if and only if the system*

$$\hat{E}\dot{\bar{x}}_i(t) = \left(\hat{A}_0 + \lambda_{ai}\hat{B}\hat{C}\right)\bar{x}_i(t) + \sum_{k=1}^{m}\hat{A}_k\bar{x}_i(t-\tau_k) \tag{27}$$

is exponentially stable $\forall\ i \in \{1,...,n\}$. Moreover we have $C(\boldsymbol{p}) = \max_{1\le i\le n}\tilde{C}(\boldsymbol{p},\lambda_{ai})$, where $\tilde{C}(\boldsymbol{p},\lambda_{ai})$ is the robust spectral abscissa of (27).

Proof. The assertions follow from the block-triangular structure of (26), with (27) appearing as a diagonal block, and from the corresponding structure of the associated eigenvalue problem. □

4.2. Decoupling for the $\mathcal{H}_\infty$ optimisation problem

Now we focus on the decomposition of the system norms, under an additional assumption, for $G(s)$ defined as the transfer function of (24) from w to z. We start by stating this assumption (recall that a matrix T is unitary if $T^*T = TT^* = I$).

Assumption 2. There exists a unitary transformation matrix T such that $TA_MT^{-1} = \Lambda_a$, with $\Lambda_a = \mathrm{diag}(\lambda_{a1},\ldots,\lambda_{an})$.

We now arrive at the main theorem.

Theorem 4.2. *If Assumption 2 is satisfied, then we can express*

$$||G(j\omega, \boldsymbol{p})||_{\mathcal{H}_\infty} = \max_{i\in\{1,..,n\}} ||\tilde{G}(j\omega, \boldsymbol{p}; \lambda_{ai})||_{\mathcal{H}_\infty} \tag{28}$$

and

$$||G(j\omega, \boldsymbol{p})||_{\mathcal{H}_2} = \sqrt{\sum_{i=1}^{n} ||\tilde{G}(j\omega, \boldsymbol{p}; \lambda_{ai})||^2_{\mathcal{H}_2}}, \tag{29}$$

where $\tilde{G}(j\omega, \boldsymbol{p}; \lambda_{ai}),\ i = 1, \ldots, n$, *is the transfer function of system*

$$\hat{E}\dot{\bar{x}}_i(t) = \left(\hat{A}_0 + \lambda_{ai}\hat{B}\hat{C}\right)\bar{x}_i(t) + \sum_{k=1}^{m} \hat{A}_k\bar{x}_i(t-\tau_k) + \hat{B}_2\bar{w}_i(t), \quad \bar{z}_i(t) = \hat{C}_2\bar{x}_i(t). \tag{30}$$

Proof. When choosing T in (25) according to Assumption 2, the transformation to (26) can be done with $Z = \Lambda_a$. Since Λ_a is a diagonal matrix, system (26) can be fully decoupled. However, input and output signals get mixed. We can express this decoupling as

$$G(s) = \hat{T}^{-1}\bar{G}(s)\hat{T}, \tag{31}$$

where $\hat{T} = T \otimes I$, with

$$\bar{G}(s) = \begin{bmatrix} \tilde{G}(s, \boldsymbol{p}; \lambda_{a1}) & \ldots & 0 \\ \vdots & \ddots & \vdots \\ 0 & \ldots & \tilde{G}(s, \boldsymbol{p}; \lambda_{an}) \end{bmatrix}. \tag{32}$$

Since $\hat{T}$ is a unitary matrix ($\hat{T}\hat{T}^* = \hat{T}^*\hat{T} = I$), induced by T being unitary from Assumption 2, we get

$$\left(\hat{T}^{-1}\bar{G}(s)\hat{T}\right)^* \left(\hat{T}^{-1}\bar{G}(s)\hat{T}\right) = \hat{T}^* \left(\bar{G}^*(s)\bar{G}(s)\right)\hat{T},$$

having the same spectrum as $\bar{G}^*(s)\bar{G}(s)$. In this way, we obtain

$$||G(s)||_{\mathcal{H}_\infty} = ||\bar{G}(s)||_{\mathcal{H}_\infty}, \quad ||G(s)||_{\mathcal{H}_2} = ||\bar{G}(s)||_{\mathcal{H}_2}.$$

The assertion regarding the $\mathcal{H}_\infty$ norm directly follows. For the $\mathcal{H}_2$ norm we get

$$\begin{aligned} ||\bar{G}(s)||_{\mathcal{H}_2} &= \sqrt{\frac{1}{2\pi}\int_{-\infty}^{+\infty} \text{trace}[\bar{G}^*(j\omega)\bar{G}(j\omega)]d\omega} \\ &= \sqrt{\sum_{i=1}^{n} \frac{1}{2\pi}\int_{-\infty}^{+\infty} \text{trace}[\tilde{G}(j\omega; \lambda_{ai})^*\tilde{G}(j\omega; \lambda_{ai})]d\omega} \end{aligned} \tag{33}$$

and the proof is complete. □

It is important to observe that equation (30) can be interpreted as the closed-loop system formed by (19)-(21), provided coupling (20) is replaced with $u_{ci}(t) = \lambda_{ai} y_{ci}(t)$. Hence, the decoupling (on which Theorem 4.2 is based) can be visualised as in Fig. 2.

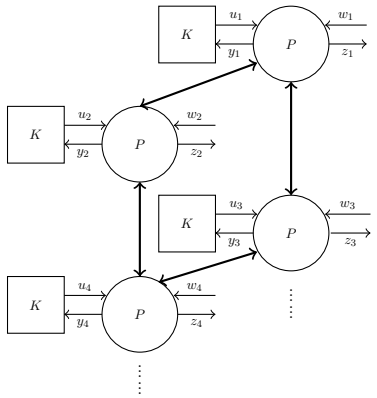

(a) Structured plant with identical subsystems and controllers.

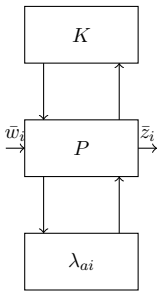

λ_{ai} are the eigenvalues of A_M, where $i \in \{1, 2, ..., n\}$.

(b) Decoupled equivalent system.

Figure 2. Decoupling of the structured plant of identical subsystems. The relation between their stability properties and their system norms of the transfer functions from w to z (and $\bar{w}$ to $\bar{z}$), are described by Theorems 4.1 and 4.2.

4.3. Discussion

The stabilisation and $\mathcal{H}_\infty$ optimisation problem of (24) can be turned into a *simultaneous* stabilisation and $\mathcal{H}_\infty$ optimisation problem of n plants of form (27), to optimise the controller parameters contained in matrix $\hat{A}_0$, using Theorems 4.1-4.2. This is particularly useful for the adopted direct optimisation approach. Recall that the dominant computational cost of evaluating the robust spectral abscissa and the strong $\mathcal{H}_\infty$ norm amounts to computing the rightmost eigenvalues of a DDAE and the imaginary axis solutions of an associated Hamiltonian eigenvalue problem respectively. In both cases the number of operations with the algorithms proposed in (Michiels, 2011) and the references therein scales with the cube of the dimension, leading to a reduction from $\mathcal{O}((n \cdot n_{cl})^3)$ to $\mathcal{O}(n \cdot (n_{cl})^3)$. Moreover, one can also interpret (30) as an uncertain system, where the uncertainty is contained in the eigenvalue parameter taking n different values. When handling this "uncertainty" using methods from robust control, similarly as done in (D'Andrea & Dullerud, 2003; Massioni & Verhaegen, 2010) for delay-free systems, there is potential to arrive at scalable design methods whose cost does not depend on the size of the network.

For the existence of the decoupling it is essential that the subsystems/nodes in $\mathcal{G}$ are identical with respect to system dynamics. We also assume that the coupling features are identical, including constant communication delays independent of the link (which are "absorbed" in the DDAE model for the subsystems, as we shall illustrate in Section 5.3). For the relation between system norms expressed in Theorem 4.2, two additional conditions are to be satisfied. First the transformation matrices used to diagonalise the adjacency matrix must be unitary. Note that this is satisfied whenever the adjacency matrix is symmetric, corresponding to symmetric bi-directional coupling, or circulant.

The (complex) Schur decomposition and spectral decomposition of a matrix coincide when the matrix is a normal matrix. Second, one has to restrict to the induced norm from w to z in the $\mathcal{H}_\infty$ problem formulation, in which the exogenous inputs and regulated outputs of the individual nodes are equally weighted.

The exploitation of the network structure, inferred from Theorem 4.1 (spectral abscissa) and first part of Theorem 4.2 ($\mathcal{H}_\infty$ norm) has been integrated in the publicly available software as an additional feature to `tds_hopt`. It relies on modifying the objective functions (9) and (13) accordingly.

4.4. Generalisations to distributed and overlapping controllers

The approach discussed in the previous subsections might be misconceived to be restricted to the case of a fully decentralised control configuration. Due to the generality of DDAEs in modelling interconnected systems, it is possible to include namely classes of distributed and overlapping controllers in the framework sketched in the beginning of Section 4. This is illustrated with the help of two examples.

Example 4.3. If we would modify system description (19)-(20) to

$$\left\{\begin{array}{rcll} \hat{E}_p\dot{x}_{pi}(t) & = & \hat{A}_{p0}x_{pi}(t)+\sum_{k=1}^{m^A}\hat{A}_{pk}x_{pi}(t-h_k^A)+\hat{B}_{p1}u_i(t)+\hat{B}_{p2}w_i(t) & \\ & & +[\hat{B}_{p3}\ 0]u_{ci}(t), & \\ 0 & = & -\xi_i(t)+u_i(t) & \\ 0 & = & -\eta_i(t)+[0\ I]u_{ci}(t) & \\ y_i(t) & = & \left[\begin{array}{c}\hat{C}_{p1}x_{pi}(t)\\ \eta_i(t)\end{array}\right], & \\ z_i(t) & = & \hat{C}_{p2}x_{pi}(t), & \\ y_{ci}(t) & = & \left[\begin{array}{c}\hat{C}_{p3}x_{pi}(t)\\ \xi_i(t)\end{array}\right], & i=1,\ldots,n, \end{array}\right. \tag{34}$$

and

$$u_{ci}(t)=\sum_{j=1}^{n}a_{Mij}y_{cj}(t),\quad i=1,\ldots,n. \tag{35}$$

where we consider the first three equations in (34) as the modified plant DDAE. Now the seemingly decentralised controller of the form (21) would correspond to an overlapping controller, whose input y_i consists not only of the original plant's output $C_{p1}x_{pi}$ but also of the weighted average of the outputs generated by neighbouring controllers. The latter can be seen from

$$\eta_i(t)=\sum_{j=1}^{n}a_{Mij}\xi_j(t)=\sum_{j=1}^{n}a_{Mij}u_j(t),$$

now we can use Theorems 4.1-4.2 to design robust controller for this example. ∘

Remark. In Section 5.3, we will consider the control of a model for the platoon of vehicles. In this application, the coupling between systems is only realised *through* the control. Such a control is of diffusive type (the controller in each vehicle is reacting on relative distances and velocities with respect to neighbouring vehicles) resulting in

overlapping controllers. We will show that the model for the closed loop system can still be turned into the form (19)-(21). ◇

Finally, the decomposition approach trivially extends to the case where the controllers communicate their state to neighbouring controllers under the condition that the interactions between different subsystems and the interactions between different controllers are described by the same network,

$$\begin{cases} \dot{x}_{ci}(t) = \hat{A}_c x_{ci}(t) + \hat{B}_{c1} y_i(t) + \hat{B}_{c2} \left(\sum_j a_{Mij} \hat{C}_{c2} x_{cj}(t-\tau) \right), \\ u_i(t) = \hat{C}_{c1} x_{ci}(t) + \hat{D}_{c1} y_i(t) + \hat{D}_{c2} \left(\sum_j a_{Mij} \hat{C}_{c2} x_{cj}(t-\tau) \right), \end{cases}$$

with τ representing a transmission delay. However, after decoupling the system, the i-th controller would become

$$\begin{cases} \dot{\bar{x}}_{ci}(t) = \hat{A}_c \bar{x}_{ci}(t) + \lambda_{ai} \hat{B}_{c2} \hat{C}_{c2} \bar{x}_{ci}(t-\tau) + \hat{B}_{c1} \bar{y}_i(t), \\ \bar{u}_i(t) = \hat{C}_{c1} \bar{x}_{ci}(t) + \lambda_{ai} D_{c2} \hat{C}_{c2} \bar{x}_{ci}(t-\tau) + \hat{D}_{c1} \bar{y}_i(t), \end{cases}$$

and hence also depend on the eigenvalue parameter. This is consistent with (Massioni & Verhaegen, 2009) for the delay-free case.

5. Numerical examples

We use some numerical examples to illustrate the network exploitation methodology presented earlier.

5.1. A system with input and coupling delays

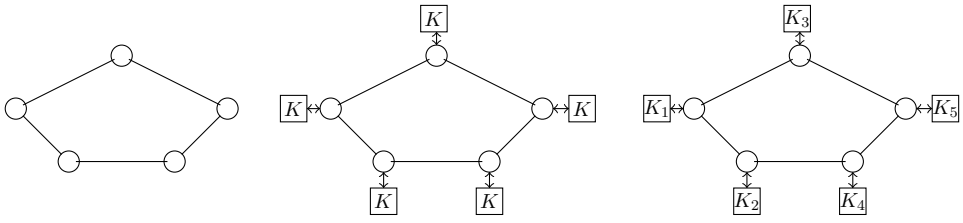

$C(\boldsymbol{p}=0) = 0.8549$ $C(\boldsymbol{p}) = -3.3672$ $C(\boldsymbol{p}) = -4.0846$

(a) No feedback (b) $u_i = Ky_i$ (c) $u_i = K_i y_i$

Figure 3. Robust spectral abscissa computed for the example system and the closed-loop subsystems.

Consider the following system with a network structure,

$$\begin{cases} \dot{x}_{pi}(t) = & \begin{bmatrix} 0 & 0.5 \\ 0.5 & -3 \end{bmatrix} x_{pi}(t) + \begin{bmatrix} 0 \\ 5 \end{bmatrix} u_i(t-0.1) + I u_{ci}(t-0.3) + \begin{bmatrix} 1 \\ 1 \end{bmatrix} w(t), \\ y_i(t) = & \begin{bmatrix} 1 & 1 \\ 0 & 1 \end{bmatrix} x_{pi}(t), \quad y_{ci}(t) = I x_{pi}(t), \quad u_{ci}(t) = \sum_{j=1}^{n} a_{Mij} x_{pj}(t), \\ z_i(t) = & I x_{pi}(t), \ i = 1, ..., 5, \end{cases} \tag{36}$$

whose adjacency matrix can be written as

$$A_M = \begin{bmatrix} 0 & 0.5 & 0.5 & 0 & 0 \\ 0.5 & 0 & 0 & 0.5 & 0 \\ 0.5 & 0 & 0 & 0 & 0.5 \\ 0 & 0.5 & 0 & 0 & 0.5 \\ 0 & 0 & 0.5 & 0.5 & 0 \end{bmatrix}. \tag{37}$$

Without control the system is unstable, with robust spectral abscissa equal to 0.8549. The generic approach of Section 3.3 is used to design decentralised controllers of the form

$$u_i(t) = K_i y_i(t),\ i = 1, ..., 5, \tag{38}$$

using the following values (generated randomly) as starting points for optimisation,

$$\begin{array}{l} \tilde{K}_1 = \begin{bmatrix} -0.8045 & 0.6966 \end{bmatrix},\ \tilde{K}_2 = \begin{bmatrix} 0.8351 & -0.2437 \end{bmatrix},\ \tilde{K}_3 = \begin{bmatrix} 0.2157 & -1.1658 \end{bmatrix}, \\ \tilde{K}_4 = \begin{bmatrix} -1.1480 & 0.1049 \end{bmatrix},\ \tilde{K}_5 = \begin{bmatrix} 0.7223 & 2.5855 \end{bmatrix}, \end{array} \tag{39}$$

leading to

$$\begin{array}{l} K_1 = \begin{bmatrix} -10.2555 & 9.2164 \end{bmatrix},\ K_2 = \begin{bmatrix} -13.9911 & 12.3932 \end{bmatrix},\ K_3 = \begin{bmatrix} -14.3001 & 12.7874 \end{bmatrix}, \\ K_4 = \begin{bmatrix} -11.3138 & 9.9052 \end{bmatrix},\ K_5 = \begin{bmatrix} -10.0127 & 9.1918 \end{bmatrix}, \end{array} \tag{40}$$

and a minimal robust spectral abscissa of -4.0846. Subsequently, using the methodology of Section 4, a static stabilising controller was designed by minimising the (robust) spectral abscissa, using the starting point (generated randomly) $\tilde{K} = [\, 0.3188 \ -1.3077]$ for optimisation, leading to

$$u_i(t) = K y_i(t) = \begin{bmatrix} -8.9481 & 7.7775 \end{bmatrix} y_i(t) \tag{41}$$

and a minimal robust spectral abscissa of -3.3672. This value is greater than that of the control law $u_i = K_i y_i$, because of the constraint that the gains are equal to each other. In Fig. 3, the robust spectral abscissa values for the subsystems and controllers are shown. Finally, the controller gains K and $K_i,\ i = 1, ..., 5$, were optimised for the (strong) $\mathcal{H}_\infty$ norm of the transfer function from w to z, to obtain $\breve{K}$ and $\breve{K}_i,\ i = 1, ..., 5$. The results are shown in Table 1, which illustrates a trade-off between performance and robustness, expressed here in terms of the robust spectral abscissa and the $\mathcal{H}_\infty$ norms respectively. As expected, we can also observe in Table 1 that the average time required for computing the objective functions have been reduced considerably by using the network structure exploitation approach (from $0.1079s$ to $0.0625s$ and from $13.676s$ to $1.7556s$ for spectral abscissa and $\mathcal{H}_\infty$ norm evaluations respectively).

Fig. 4 shows the convergence of the optimisation problems through HANSO iterations for the results given in Table 1. Due to the non-convexity of the problem, different starting points could lead to different results and therefore different convergence profiles (including the number of iterations or function evaluations). In the optimisation process, HANSO might perform multiple objective function evaluations within one iteration. For more details on the controllers and other results presented in this paper,

[1] Average time taken (MATLAB tic-toc) for the objective function evaluation in the optimisation process.

Table 1. Results obtained for simple numerical example using the two approaches

Simple numerical example	Objective function	$\mathcal{H}_\infty$ norm	Spectral abscissa	Function evaluations (No.)	Function evaluation time[1](s)
No feedback	—	∞	0.8549	—	—
$u_i = Ky_i$	Robust spectral abscissa ($\alpha = 1$)	3.2246	-3.3672	326	0.0625↓
$u_i = \breve{K}y_i$	Strong $\mathcal{H}_\infty$ norm ($\alpha = 0$)	2.7661↓	-2.1936↑	38	1.7556↓
$u_i = K_i y_i$	Robust spectral abscissa ($\alpha = 1$)	2.8662	-4.0846	432	0.1079↑
$u_i = \breve{K}_i y_i$	Strong $\mathcal{H}_\infty$ norm ($\alpha = 0$)	2.7580↓	-2.6168↑	53	13.676↑

please refer to the complementary software package (Dileep & Michiels, 2018). The tests were performed using an Intel® Core™i7-6820HQ CPU at 2.7 GHz with 8GB RAM.

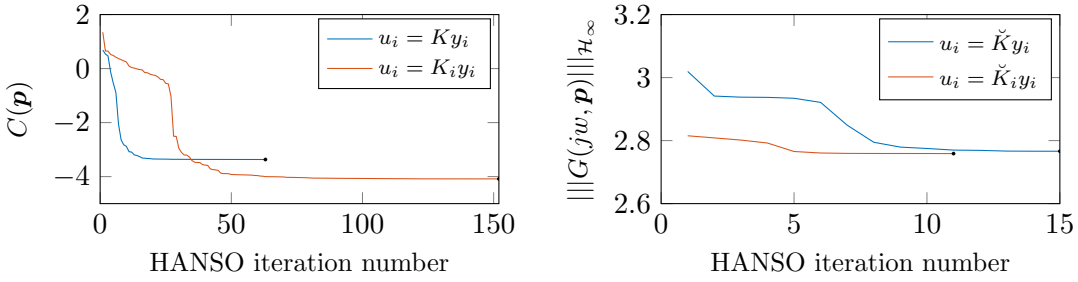

(a) Robust sectral abscissa optimisation.

(b) Strong $\mathcal{H}_\infty$ norm optimisation.

Figure 4. Convergence profile of the optimisation process for (a) robust spectral abscissa ($\alpha = 1$) and (b) strong $\mathcal{H}_\infty$ norm ($\alpha = 0$) of the simple numerical example.

5.2. A neutral type time-delay system

Let us consider a neutral type time-delay system

$$\begin{cases} \begin{bmatrix} 0 & 1 \\ 0.5 & 2 \end{bmatrix} \dot{x}_{pi}(t) + \begin{bmatrix} 0 & 0 \\ 0.2 & 1 \end{bmatrix} \dot{x}_{pi}(t-0.2) = \begin{bmatrix} 1 & -0.5 \\ 0 & 2 \end{bmatrix} x_{pi}(t) \\ \qquad\qquad + \begin{bmatrix} 1 \\ 0 \end{bmatrix} u_i(t-0.5) + Iu_{ci}(t-0.3) + \begin{bmatrix} 1 \\ 1 \end{bmatrix} w(t), \\ y_i(t) = \begin{bmatrix} 1 & 1 \\ 0 & 1 \end{bmatrix} x_{pi}(t), \quad y_{ci}(t) = Ix_{pi}(t), \quad u_{ci}(t) = \sum_{j=1}^{n} a_{Mij} x_{pj}(t), \\ z_i(t) = Ix_{pi}(t), \ i = 1, ..., 5, \end{cases} \tag{42}$$

whose adjacency matrix is the same as in (37). Without control, this system is unstable with a robust spectral abscissa equal to 0.7927. However, using the approach of network structure exploitation presented in Section 4, we were able to find a stablising controller (optimising with $\alpha = 1$) $\hat{K} = \begin{bmatrix} -0.8420 & -3.2729 \end{bmatrix}$ and subsequently a robust controller (optimising with $\alpha = 0$) $\bar{K} = \begin{bmatrix} -1.6118 & -2.5654 \end{bmatrix}$. The results corresponding to robust spectral abscissa and strong $\mathcal{H}_\infty$ norm are given in Table 2.

In this example, the results have not been compared to the design approach using

[2]Average time taken (MATLAB tic-toc) for the objective function evaluation in the optimisation process.

Table 2. Results obtained for neutral type time-delay system

Neutral type system	Objective function	$\mathcal{H}_\infty$ norm	Spectral abscissa	Function evaluations (No.)	Function evaluation time[2](s)
No feedback	—	∞	0.7927	—	—
$u_i = \hat{K} y_i$	Robust spectral abscissa ($\alpha = 1$)	8.5494	-0.4870	96	0.80073
$u_i = \bar{K} y_i$	Strong $\mathcal{H}_\infty$ norm ($\alpha = 0$)	6.3943$\downarrow$	$-0.3719\uparrow$	48	4.3647

structural constraints in the controller. The resulting conclusions were not found to qualitatively differ from that presented in the previous example.

5.3. A consensus type problem

We consider a car-following problem involving n vehicles. We use a simplified vehicle model from (Zheng, Li, Wang, Wang, & Li, 2014),

$$\begin{aligned} \dot{s}_i(t) &= v_i(t), \\ \dot{v}_i(t) &= f_i(t), \\ \dot{f}_i(t) &= -\frac{1}{\tau_c} f_i(t) + u_i(t - \breve{\tau}), \end{aligned} \tag{43}$$

where $f_i(t)$, $v_i(t)$ and $s_i(t)$ represents the acceleration force, velocity and position of the vehicle i at the time t. The time constant of the vehicle engine (in (Stankovic, Stanojevic, & Siljak, 2000; Zheng et al., 2014), and references therein) is denoted by $\tau_c (= 0.4)$ and the overall delay in the control is denoted by $\breve{\tau} (= 0.8s)$. We consider position and velocity as outputs,

$$y_i(t) = \begin{bmatrix} s_i(t) & v_i(t) \end{bmatrix}^{\mathrm{T}}. \tag{44}$$

This system can be rewritten in state space form (with $\psi_i = \begin{bmatrix} s_i & v_i & f_i \end{bmatrix}^{\mathrm{T}}$) as

$$\dot{\psi}_i(t) = \underbrace{\begin{bmatrix} 0 & 1 & 0 \\ 0 & 0 & 1 \\ 0 & 0 & -\frac{1}{\tau_c} \end{bmatrix}}_{A_g} \psi_i(t) + \underbrace{\begin{bmatrix} 0 \\ 0 \\ 1 \end{bmatrix}}_{B_g} u_i(t - \breve{\tau}), \quad y_i(t) = \underbrace{\begin{bmatrix} 0 & 1 & 0 \\ 0 & 0 & 1 \end{bmatrix}}_{C_g} \psi_i(t). \tag{45}$$

Note that, without control, the stationary solutions of (43) can be parameterised by

$$\begin{aligned} s_i(t) &= s_{ki} + v_k \, t, \\ v_i(t) &= v_k, \\ f_i(t) &= 0, \quad v_k, s_{ki} \in \mathbb{R}, \end{aligned} \tag{46}$$

where s_{ki} is the desired zero-velocity position and v_k is the desired velocity. We consider a network of n nodes, each node corresponding to a system/vehicle, and $R \geq 0$ virtual nodes, indexed by $i \in \{n+1, ..., n+R\}$. The dynamics of the virtual nodes, which are

used to generate external reference trajectories (e.g., a leader), can be written as

$$\begin{aligned} \dot{\psi}_i(t) &= A_g \psi_i(t), \\ y_i(t) &= C_g \psi_i(t) \quad \forall\ i = n+1, ..., n+R. \end{aligned} \tag{47}$$

We consider identical controllers in each vehicle that react on differences in position and velocities with respect to neighbours (possibly including external reference generated by the virtual nodes), more precisely we let[3]

$$\begin{aligned} u_i(t) =& K_1 \sum_{\substack{j=1 \\ j\neq i}}^{n+R} a_{Mij} \left(s_j(t) - s_i(t) - d_{ij} \right) \\ &+ K_2 \sum_{\substack{j=1 \\ j\neq i}}^{n+R} a_{Mij} \left(v_j(t) - v_i(t) \right),\ \forall\ i \in \{1, ..., n\}, \end{aligned} \tag{48}$$

where we assume $a_{Mij} \geq 0,\ \ i = 1 \ldots, n,\ j = 1, \ldots, , n+R$ and

$$\sum_{j=1}^{n+R} a_{Mij} = 1, \quad i = 1, \ldots, n.$$

The above set of equations describes diffusive coupling between systems, where d_{ij} is the constant prescribed reference distance between the vehicles i and j.

5.3.1. Standard form

Let the function $t \in \mathbb{R} \to x_{ri}(t)$ be a reference trajectory for system i such that

$$\begin{array}{lll} \dot{x}_{ri}(t) & = A_g x_{ri}(t) & i = 1, \ldots, n+R, \\ x_{ri}(t) & = \psi_i(t), & i = n+1, ..., n+R, \\ x_{ri}(t) - x_{rj}(t) & = \begin{bmatrix} d_{ij} & 0 & 0 \end{bmatrix}^{\mathrm{T}} & i, j \in 1, ..., n+R,\ t \geq 0. \end{array} \tag{49}$$

If we consider the new state as $\bar{\psi}_i(t) = \psi_i(t) - x_{ri}(t)$ then we can reformulate (45) as

$$\begin{aligned} \dot{\bar{\psi}}_i(t) &= A_g \bar{\psi}_i(t) + B_g u_i(t - \breve{\tau}), \\ \bar{y}_i(t) &= C_g \bar{\psi}_i(t), \end{aligned} \tag{50}$$

since by definition $\psi_i - x_{ri} = 0, i = n+1, ..., n+R$, control law (48) becomes

$$u_i(t) = K \underbrace{\left(\sum_{j=1}^{n} a_{Mij} \left(\bar{y}_j(t) - \bar{y}_i(t) \right) - \sum_{j=n+1}^{n+R} a_{Mij} \bar{y}_i(t) \right)}_{\sum_{j=1}^{n} a_{Mij} \bar{y}_j(t) - \bar{y}_i(t)},\ i = 1, \ldots, n. \tag{51}$$

[3]In order to simplify notations and shorten the equations, we denote by $u = K(s)y$ the application of a feedback controller coupling $y(t)$ to $u(t)$, whose transfer function is given by $K(s)$.

with $K(s) = [K_1(s)\ K_2(s)]$. Unlike in the standard form (19)-(21), system (50)-(51) features input delay as well as controllers acting (partly) on differences in outputs. However, using dummy variables (ν and ξ) we can rewrite (51) as

$$\begin{cases} \dot{\bar{\psi}}_i(t) & = A_g\bar{\psi}_i(t) + B_g\nu_i(t-\breve{\tau}) & + w(t) \\ 0 & = -\nu_i(t) & + u_i(t) \\ 0 & = -\xi_i(t) - C_g\bar{\psi}_i(t) & + u_{ci}(t) \\ \bar{y}_i(t) & = \xi_i(t) & \\ y_{ci}(t) & = C_g\bar{\psi}_i(t) & \\ z(t) & = \begin{bmatrix} 0 & 1 & 0 \end{bmatrix}\bar{\psi}_i(t) & \end{cases}, \tag{52}$$

which is of form (19) with $x_{pi} = \left[\bar{\psi}_i^{\mathrm{T}}(t) \quad \nu_i^{\mathrm{T}}(t) \quad \xi_i^{\mathrm{T}}(t)\right]^{\mathrm{T}}$, while the coupling becomes

$$u_{ci}(t) = \sum_{j=1}^{n} a_{Mij} y_{cj}(t),\ i = 1, \ldots, n. \tag{53}$$

The feedback is described in the Laplace domain by

$$u_i(s) = K(s)\bar{y}_i(s),\ i = 1, \ldots, n, \tag{54}$$

where $K(s)$ is the transfer function of the dynamic controller. We allow virtual nodes, therefore, it is possible that $\sum_{j=1}^{n} a_{Mij} \leq 1$.

5.3.2. Ring topology: consensus problem

For a ring configuration there are no virtual nodes ($R = 0$), and the adjacency matrix is described by

$$A_{M1} = \begin{bmatrix} 0 & \ldots & 0 & 1 \\ 1 & \ldots & 0 & 0 \\ \vdots & \ddots & \vdots & \vdots \\ 0 & \ldots & 1 & 0 \end{bmatrix} \tag{55}$$

for unidirectional coupling, and by

$$A_{M2} = \begin{bmatrix} 0 & 0.5 & 0 & \ldots & 0 & 0.5 \\ 0.5 & 0 & 0.5 & \ldots & 0 & 0 \\ 0 & 0.5 & 0 & \ldots & 0 & 0 \\ \vdots & \vdots & \vdots & \ddots & \vdots & \vdots \\ 0 & 0 & 0 & \ldots & 0 & 0.5 \\ 0.5 & 0 & 0 & \ldots & 0.5 & 0 \end{bmatrix} \tag{56}$$

for bidirectional coupling where the control is based on the average of the deviation of speed and velocity with respect to the preceding and following vehicle.

Without virtual nodes, the row-sum condition

$$\sum_{j=1}^{n} a_{Mij} = 1, \quad i = 1, \ldots, n$$

is satisfied, hence, the adjacency matrix always has an eigenvalue equal to one (Michiels & Nijmeijer, 2009). As shown in the appendix this implies that, independent of the control, the closed-loop system (52)-(54) always has a double eigenvalue at zero. This has a natural interpretation. We are dealing with a *consensus problem*, where every solution of form (46) with v_{ki} independent of i and $s_{kj} - s_{ki} = d_{ij}$, correspond to a stationary solution. If the remaining eigenvalues are in the open left half plane, the reached consensus with respect to speed and the offset of the position component of the limit solution depend on the initial condition and disturbances.
As a consequence of the above, the robust spectral abscissa for the closed-loop system is always greater or equal to zero. However, to maximise the speed in which a consensus is reached we optimise instead

$$\begin{aligned} \breve{C}(\boldsymbol{p};\boldsymbol{\tau}) &:= \lim_{\epsilon \to 0+} \sup_{\boldsymbol{\tau}_\epsilon \in \mathcal{B}(\boldsymbol{\tau},\epsilon)} \breve{c}(\boldsymbol{p};\boldsymbol{\tau}_\epsilon), \\ \breve{c}(\boldsymbol{p}) &= \max_{\substack{1 \le i \le n \\ i \ne k}} \left\{ \sup_{\lambda \in \mathbb{C}} \{ \Re(\lambda) : \ \det \tilde{\Delta}(\lambda; \lambda_{ai}) = 0 \} \right\}, \end{aligned} \tag{57}$$

where $\tilde{\Delta}$ is the characteristic matrix of (27) and k is such that $\lambda_{ak} = 1$. When optimising the above modified spectral abscissa for plant (52)-(54) and (56), with $n = 5$ and controller order $n_c = 1$, we obtain

$$\begin{cases} \dot{x}_{ci}(t) = \begin{bmatrix} -86.2588 \end{bmatrix} x_{ci}(t) + \begin{bmatrix} -249.5680 & -48.9190 \end{bmatrix} \bar{y}_i(t), \\ u_i(t) = \begin{bmatrix} -8.0038 \end{bmatrix} x_{ci}(t) + \begin{bmatrix} -23.8468 & -4.7045 \end{bmatrix} \bar{y}_i(t). \end{cases} \tag{58}$$

The corresponding rightmost eigenvalues are visualised in Fig. 5. In general, defining any exogenous inputs and regulated outputs results in the strong $\mathcal{H}_\infty$ norm for the closed-loop system to be equal to infinity, due to the fact that the system does not settle back to the original stationary solution after a perturbation.

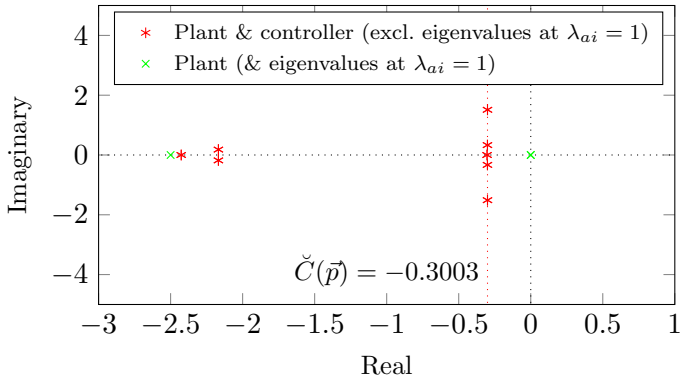

Figure 5. Optimised spectrum plotted for the consensus problem of five vehicles in a ring topology with bidirectional communication links.

5.3.3. Linear topology: mixed consensus/reference tracking problem

Let us now consider a linear platoon of vehicles. In case of unidirectional coupling, a special treatment should be given to the first vehicle, which we can solve by adding a virtual node ($R \neq 0$) that serves as a generator of the reference trajectory for this vehicle. In this way we arrive at elements a_{Mij} contained in

$$A_{M3} = \begin{bmatrix} 0 & \dots & 0 & 0 \\ 1 & \dots & 0 & 0 \\ \vdots & \ddots & \vdots & \vdots \\ 0 & \dots & 1 & 0 \end{bmatrix}. \tag{59}$$

All eigenvalues of A_{M3} are equal to zero, implying that the decomposition approach leads to identical subsystems of form (30). The interpretation is as follows: for each vehicle we have to solve the same control problem of tracking the outputs generated by preceding vehicle. For bidirectional coupling, a special treatment should also be given to the last vehicle, in order to preclude any asymmetry, and the adjacency matrix takes the form

$$A_{M4} = \begin{bmatrix} 0 & 0.5 & 0 & \dots & 0 & 0 \\ 0.5 & 0 & 0.5 & \dots & 0 & 0 \\ 0 & 0.5 & 0 & \dots & 0 & 0 \\ \vdots & \vdots & \vdots & \ddots & \vdots & \vdots \\ 0 & 0 & 0 & \dots & 0 & 0.5 \\ 0 & 0 & 0 & \dots & 0.5 & 0 \end{bmatrix}, \tag{60}$$

where there exist virtual nodes ($R \neq 0$) communicating with the first and last nodes.

Table 3. Strong $\mathcal{H}_\infty$ norm optimisation.

Example	Feedback control	Robust spectral abscissa	Strong $\mathcal{H}_\infty$ norm
Platoon of four vehicles	$u_i = K(s)\bar{y}_i$	-0.2103	20.5379
	$u_i = \check{K}(s)\bar{y}_i$	$-0.1648\uparrow$	$8.2504\downarrow$

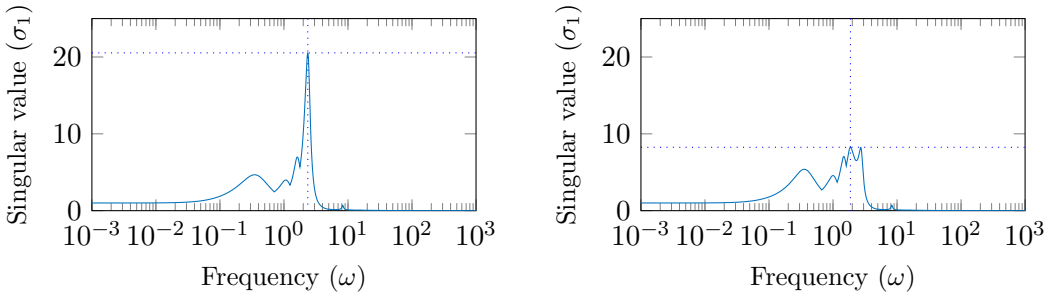

(a) $u_i = K(s)\bar{y}_i$. (b) $u_i = \check{K}(s)\bar{y}_i$.

Figure 6. The maximum singular value plot of the transfer function from w to z for the structured closed-loop systems before and after the strong $\mathcal{H}_\infty$ norm optimisation of the controller parameters.

Table 4. Zero-velocity positions (s_{ki} as in (46)).

Vehicle "i"	$t \in [0, 10)$	$t \in [10, 34)$	$t \geq 34$
1	10	8	8
2	20	16	16
2b	-	-	24
3	30	32	32
4	40	40	40

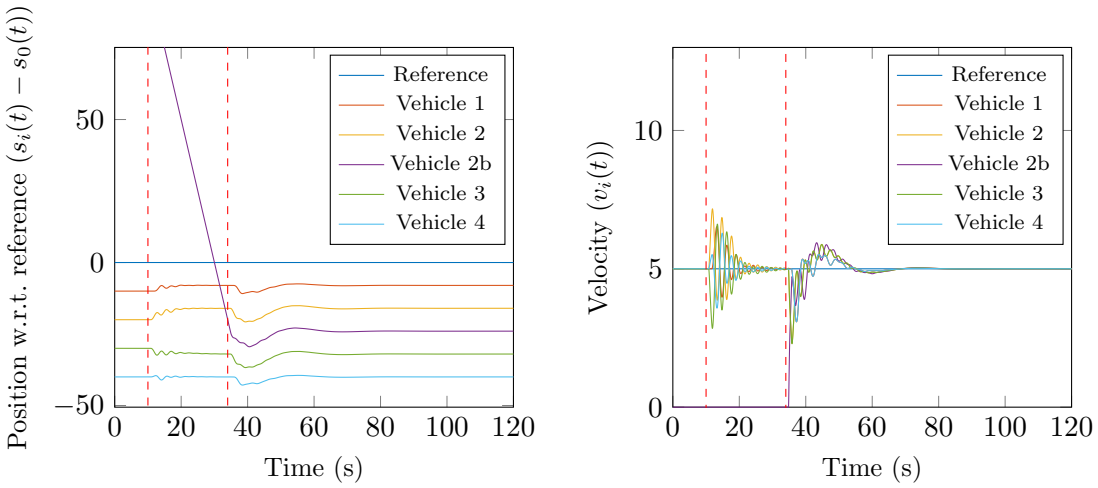

(a) Relative positions of the vehicles in linear platoon.

(b) Velocities of the vehicles in linear platoon.

Figure 7. MATLAB simulation of a new vehicle merging into a platoon of 4 vehicles, where the vehicle dynamics is adopted from the closed-loop system (52)-(54). The platoon makes way for the new vehicle at 10s and Vehicle 2b joins the platoon at 34s.

We consider $n = 4$ vehicles and we first design controller $K(s)$ in (51) as a dynamic LTI controller of order 3 minimising the (robust) spectral abscissa, resulting in a spectral abscissa of -0.2103. Subsequently, we use this controller as starting point to optimise the (strong) $\mathcal{H}_\infty$ norm of the transfer function from w to z for the system in (52) and we obtain the robust controller $\breve{K}(s)$. The robust spectral abscissa and strong $\mathcal{H}_\infty$ norm values obtained are shown in Table 3. The maximum singular value plots of the transfer function from w to z for the structured closed-loop systems ($u_i = K(s)\bar{y}_i$ and $u_i = \breve{K}(s)\bar{y}_i$) are shown in Fig. 6.

Finally, we consider the bidirectional coupling case and controller $\breve{K}(s)$ designed in this subsection, to show the effect of adding a node. By switching the off-sets of the reference trajectories and the relative distances d_{ij} appropriately, as in Table 4, we simulate the merging of a new car in a platoon of 4 vehicles. Note that at the level of equations (50), such switches correspond to jumps in the state-variables perturbing the equilibrium. The results are visualised in Fig. 7a and Fig. 7b.

6. Conclusion

The problem of the decentralised/overlapping controller design for systems with time-delays has been addressed in this article. A generic technique for LTI systems modelled by DDAEs is presented, based on imposing sparsity constraints in the controller parameterisation, and a structure exploiting approach is proposed for networks of identical systems and local controllers. By means of a case-study inspired by the control of a

platoon of vehicles, the applicability to consensus type problems is shown, while also illustrating the flexibility of the modelling framework and control technique.

The proposed direct optimization approach is a non-conservative technique for controller design in the frequency domain, grounded in necessary and sufficient stability conditions. The approach is flexible with respect to the structure that can be imposed on the controller. Issues related non-convexity and non-smoothness of the optimisation problem in general (especially for $\mathcal{H}_\infty$ norm) are still existent as in the centralised setting. The non-smoothness is handled by using the special algorithm HANSO. With respect to the non-convexity, the algorithm can converge to local optima which are not global. The latter is mitigated by considering sufficiently large number of randomly generated (or user specified) starting points for the optimisation problem.

A main direction for future research consists of further exploiting the decomposition for classes of applications, aiming at a computational cost barely depending on the network size. One of the starting points is the combination of the presented results with the computation and optimization of structured pseudo-spectral abscissae, which relate to *necessary and sufficient* robust stability conditions for broad classes of delay systems (see, e.g., (Borgioli & Michiels, 2018)).

Acknowledgements

This work was supported by the project C14/17/072 of the KU Leuven Research Council, by the project G0A5317N of the Research Foundation-Flanders (FWO - Vlaanderen), and by the project UCoCoS funded by the European Union's Horizon 2020 research and innovation programme under the Marie Sklodowska-Curie Grant Agreement No 675080.

References

Alavian, A., & Rotkowitz, M. (2015). On the pole selection for h-infinity optimal decentralized control. In *2015 american control conference (acc)* (p. 5471-5476).

Alavian, A., & Rotkowitz, M. C. (2013). Q-parametrization and an SDP for H-infinity-optimal decentralized control. *IFAC Proceedings Volumes*, *46*(27), 301 - 308.

Apkarian, P., & Noll, D. (2006, January). Non-smooth H-infinity synthesis. *IEEE Transactions on Automatic Control*, *51*(1), 71-86.

Apkarian, P., & Noll, D. (2017, July). Structured H-infinity control of infinite dimensional systems. *International Journal of Robust and Nonlinear Control (to appear)*.

Borgioli, F., & Michiels, W. (2018, June). Computing distance to instability for delay systems with uncertainities in the system matrices and in the delay terms. In *17th annual European Control Conference (ECC)*.

Boyd, S., Balakrishnan, V., & Kabamba, P. (1989, September 01). A bisection method for computing the h-infinity norm of a transfer matrix and related problems. *Mathematics of Control, Signals and Systems*, *2*(3), 207–219.

Bruinsma, N. A., & Steinbuch, M. (1990). A fast algorithm to compute the h-infinity-norm of a transfer function matrix. *Systems & Control Letters*, *14*(4), 287 - 293.

Burke, J., Henrion, D., Lewis, A., & Overton, M. (2006). HIFOO - a matlab package for fixed-order controller design and H-infinity optimization. *IFAC Proceedings Volumes*, *39*(9), 339 - 344. (5th IFAC Symposium on Robust Control Design)

D'Andrea, R., & Dullerud, G. E. (2003). Distributed control design for spatially interconnected systems. *IEEE Transactions on automatic control*, *48*(9), 1478–1495.

Dileep, D., & Michiels, W. (2018). *tds_hopt-nse, a software tool for structured controller design for DDAEs with network structure exploitation.* Retrieved from `http://twr.cs.kuleuven.be/research/software/delay-control/tds_hopt-nse.zip`

Dileep, D., Michiels, W., Hetel, L., & Richard, J. P. (2018, June). Design of robust structurally constrained controllers for MIMO plants with time-delays. In *17th annual European Control Conference (ECC).*

Fridman, E. (2014). *Introduction to time-delay systems: Analysis and control.* Springer International Publishing.

Gahinet, P., & Apkarian, P. (1994). A linear matrix inequality approach to $\mathcal{H}_\infty$ control. *International Journal of Robust and Nonlinear Control*, *4*(4), 421–448.

Gumussoy, S., & Michiels, W. (2011). Fixed-order H-infinity control for interconnected systems using delay differential algebraic equations. *SIAM Journal on Control and Optimization*, *49*(5), 2212-2238.

Hale, J. K., & Verduyn Lunel, S. M. (2002). Strong stabilization of neutral functional differential equations. *IMA Journal of Mathematical Control and Information*, *19*, 5-23.

Lunze, J. (1992). *Feedback control of large scale systems.* Prentice-Hall.

Massioni, P., & Verhaegen, M. (2009). Distributed control for identical dynamically coupled systems: A decomposition approach. *IEEE Transactions on Automatic Control*, *54*(1), 124–135.

Massioni, P., & Verhaegen, M. (2010). A full block s-procedure application to distributed control. In *American Control Conference (ACC), 2010* (pp. 2338–2343).

McMillan, G. K. (2012). Industrial applications of pid control. In R. Vilanova & A. Visioli (Eds.), *PID control in the third millennium: Lessons learned and new approaches* (pp. 415–461). Springer London.

Meyer, C. (2000). *Matrix analysis and applied linear algebra:.* Society for Industrial and Applied Mathematics.

Michiels, W. (2011, November). Spectrum-based stability analysis and stabilisation of systems described by delay differential algebraic equations. *IET Control Theory Applications*, *5*(16), 1829-1842.

Michiels, W., Hilhorst, G., Pipeleers, G., Vyhlídal, T., & Swevers, J. (2017, December). Reduced modelling and fixed-order control of delay systems applied to a heat exchanger. *IET Control Theory & Applications*, *11*, 3341-3352(11).

Michiels, W., & Nijmeijer, H. (2009). Synchronization of delay-coupled nonlinear oscillators: An approach based on the stability analysis of synchronized equilibria. *Chaos: An Interdisciplinary Journal of Nonlinear Science*, *19*(3), 033110.

Michiels, W., Vyhlídal, T., Ziték, P., Nijmeijer, H., & Henrion, D. (2009). Strong stability of neutral equations with an arbitrary delay dependency structure. *SIAM Journal on Control and Optimization*, *48*(2), 763-786.

Olfati-Saber, R., & Murray, R. M. (2004). Consensus problems in networks of agents with switching topology and time-delays. *IEEE Transactions on Automatic Control*, *49*(9), 1520-1533.

Overton, M. L. (2009). HANSO: a hybrid algorithm for non-smooth optimization. *Computer Science, New York University*.

Ozer, S. M., & Iftar, A. (2015). Decentralized controller design for time-delay systems by optimization. *IFAC-PapersOnLine*, *48*(12), 462 - 467.

Pecora, L. M., & Carroll, T. L. (1998, March). Master stability functions for synchronized coupled systems. *Phys. Rev. Lett.*, *80*, 2109–2112.

Shi, X. Q., Davison, D. E., Kwong, R., & Davison, E. J. (2016, June). Optimized decentralized control of large scale systems. In *2016 12th IEEE International Conference on Control and Automation (ICCA)* (p. 127-134).

Siljak, D. (1991). *Decentralized control of complex systems.* Elsevier Science.

Stankovic, S. S., Stanojevic, M. J., & Siljak, D. D. (2000, September). Decentralized overlapping control of a platoon of vehicles. *IEEE Transactions on Control Systems Technology*, *8*(5), 816-832.

Zheng, Y., Li, S. E., Wang, J., Wang, L. Y., & Li, K. (2014, October). Influence of information flow topology on closed-loop stability of vehicle platoon with rigid formation. In *17th International IEEE Conference on Intelligent Transportation Systems (ITSC)* (p. 2094-2100).

Appendix A. Well posedness of the systems considered

In this section of appendix we refer to the Assumption 3.1 in (Gumussoy & Michiels, 2011) applied to the closed loop system (5) which reads as $\det(\tilde{U}^{\mathrm{T}} A_0 \tilde{V}) \neq 0$ where the columns of matrix $\tilde{U}$ and $\tilde{V}$ are the (minimal) basis for the right and left nullspace of E respectively,

$$\tilde{U}^{\mathrm{T}} E = 0 \text{ and } E\tilde{V} = 0.$$

This can be rephrased as the Assumption 1 mentioned in this paper, using the theorem below.

Theorem A.1. *Matrix $U^T(A_{p0} + B_{p1}D_cC_{p1})V$ being non-singular is equivalent to $\tilde{U}^T A_0 \tilde{V}$ being non-singular.*

Proof. We consider the following relations for U and V with $\tilde{U}$ and $\tilde{V}$ respectively,

$$\tilde{U}^{\mathrm{T}} = \begin{bmatrix} U^{\mathrm{T}} & 0 & 0 & 0 & 0 \\ 0 & I & 0 & 0 & 0 \\ 0 & 0 & I & 0 & 0 \\ 0 & 0 & 0 & 0 & I \end{bmatrix}; \qquad \tilde{V} = \begin{bmatrix} V & 0 & 0 & 0 \\ 0 & I & 0 & 0 \\ 0 & 0 & I & 0 \\ 0 & 0 & 0 & 0 \\ 0 & 0 & 0 & I \end{bmatrix}. \tag{A1}$$

Using (23) and (A1) we can write the expression

$$M := \tilde{U}^{\mathrm{T}} A_0 \tilde{V} = \left[\begin{array}{c|ccc} U^{\mathrm{T}} A_{p0} V & U^{\mathrm{T}} B_{p1} & U^{\mathrm{T}} B_{p2} & 0 \\ \hline C_{p1} V & 0 & 0 & -I \\ 0 & 0 & -I & 0 \\ 0 & -I & 0 & D_c \end{array}\right]. \tag{A2}$$

The matrix $\tilde{U}^{\mathrm{T}} A_0 \tilde{V}$ being invertible is equivalent to the block

$$X := \begin{bmatrix} 0 & 0 & -I \\ 0 & -I & 0 \\ -I & 0 & D_c \end{bmatrix} \tag{A3}$$

and the Schur complement (M/X) of the block X of the matrix M being invertible. We can see that X is always invertible (independent of D_c) due to its structure. M/X is invertible if

$$\begin{aligned} M/X &= U^{\mathrm{T}} A_{p0} V - \begin{bmatrix} U^{\mathrm{T}} B_{p1} & U^{\mathrm{T}} B_{p2} & 0 \end{bmatrix} X^{-1} \begin{bmatrix} C_{p1} V \\ 0 \\ 0 \end{bmatrix} \\ &= U^{\mathrm{T}} A_{p0} V + U^{\mathrm{T}} B_{p1} D_c C_{p1} V \end{aligned} \tag{A4}$$

is invertible. The proof is complete. □

Appendix B. Vehicular platoon in a ring network topology

In this section of the appendix we show that the closed-loop system (52)-(54) in a ring configuration has double zero eigenvalues, independent of the control.

Theorem B.1. *There always exist two zero eigenvalues for the closed-loop system of a platoon of vehicles (52) in ring network topology and their controller(s), irrespective of the controller parameters and the number of vehicles.*

Proof. The closed-loop system can be written in the DDAE form of (22) for $w \equiv 0$ using (21) and (52). For this, we consider the new state $x_i(t) = [\bar{\psi}_{pi}^{\mathrm{T}}(t)\ \nu_i^{\mathrm{T}}(t)\ \xi_i^{\mathrm{T}}(t)\ x_{ci}^{\mathrm{T}}(t)]^{\mathrm{T}}$,

$$\begin{aligned} &\begin{bmatrix} I & 0 & 0 & 0 \\ 0 & 0 & 0 & 0 \\ 0 & 0 & 0 & 0 \\ 0 & 0 & 0 & I \end{bmatrix} \dot{x}_i(t) = \begin{bmatrix} A_g & 0 & 0 & 0 \\ 0 & -I & \hat{D}_c & \hat{C}_c \\ -C_g & 0 & -I & 0 \\ 0 & 0 & \hat{B}_c & \hat{A}_c \end{bmatrix} x_i(t) + \begin{bmatrix} 0 & B_g & 0 & 0 \\ 0 & 0 & 0 & 0 \\ 0 & 0 & 0 & 0 \\ 0 & 0 & 0 & 0 \end{bmatrix} x_i(t-\breve{\tau}) + \begin{bmatrix} 0 \\ 0 \\ I \\ 0 \end{bmatrix} u_{ci}(t), \\ &y_{ci}(t) = \begin{bmatrix} C_g & 0 & 0 & 0 \end{bmatrix} x_i(t). \end{aligned} \tag{B1}$$

Now we can bring the above equation, supplemented with (53) in a decoupled form as in (27), after the use of an appropriate transformation matrix,

$$\begin{aligned} \begin{bmatrix} I & 0 & 0 & 0 \\ 0 & 0 & 0 & 0 \\ 0 & 0 & 0 & 0 \\ 0 & 0 & 0 & I \end{bmatrix} \dot{\bar{x}}_i(t) = &\left(\begin{bmatrix} A_g & 0 & 0 & 0 \\ 0 & -I & \hat{D}_c & \hat{C}_c \\ -C_g & 0 & -I & 0 \\ 0 & 0 & \hat{B}_c & \hat{A}_c \end{bmatrix} + \lambda_{ai} \begin{bmatrix} 0 & 0 & 0 & 0 \\ 0 & 0 & 0 & 0 \\ C_g & 0 & 0 & 0 \\ 0 & 0 & 0 & 0 \end{bmatrix} \right) \bar{x}_i(t) \\ &+ \begin{bmatrix} 0 & B_g & 0 & 0 \\ 0 & 0 & 0 & 0 \\ 0 & 0 & 0 & 0 \\ 0 & 0 & 0 & 0 \end{bmatrix} \bar{x}_i(t-\breve{\tau}), \end{aligned} \tag{B2}$$

for $i \in \{1, ..., n\}$. Based on the assumption that the system has a ring network topology, A_M contains an eigenvalue $1\ \forall\ n \in \mathbb{N} \setminus \{1\}$ at some value $i = k$ $(\lambda_{ak} = 1)$, where $\mathbb{N}$

represents the set of all natural numbers. The k-th subsystem then takes the form

$$\begin{bmatrix} I & 0 & 0 & 0 \\ 0 & 0 & 0 & 0 \\ 0 & 0 & 0 & 0 \\ 0 & 0 & 0 & I \end{bmatrix} \dot{\bar{x}}_k(t) = \begin{bmatrix} A_g & 0 & 0 & 0 \\ 0 & -I & \hat{D}_c & \hat{C}_c \\ \boxed{0} & 0 & -I & 0 \\ 0 & 0 & \hat{B}_c & \hat{A}_c \end{bmatrix} \bar{x}_k(t) + \begin{bmatrix} 0 & B_g & 0 & 0 \\ 0 & 0 & 0 & 0 \\ 0 & 0 & 0 & 0 \\ 0 & 0 & 0 & 0 \end{bmatrix} \bar{x}_k(t - \check{\tau}). \tag{B3}$$

The above equation shows that the spectrum of system matrix A_g, which contains a double eigenvalue at zero, is part of the spectrum of the closed-loop system. The proof is complete. □

Remark. Theorem B.1 also holds true for other network typologies whose adjacency matrix has at least one eigenvalue equal to 1. ◇